Cross-Linking of Myosin Subfragment 1 and Heavy Meromyosin by Use of Vanadate and a Bis(adenosine 5′-triphosphate) Analogue†

Keith B. Munson, Michael J. Smerdon, and Ralph G. Yount*

Biochemistry/Biophysics Program, Institute of Biological Chemistry and Department of Chemistry, Washington State University, Pullman, Washington 99164-4630

Received February 11, 1986; Revised Manuscript Received July 25, 1986

ABSTRACT: The synthesis of a divalent ATP analogue [3,3′-dithiobis[3′(2′)-*O*-[6-(propionylamino)hexanoyl]adenosine 5′-triphosphate] ($bis_{22}ATP$)] is described in which two molecules of ATP are linked via esterification of their 3′(2′)-hydroxyls to the linear dicarboxylic acid 3,3′-dithiobis[*N*-(5-carboxypentyl)-propionamide] [$[HO_2C(CH_2)_5NHC(O)(CH_2)_2S-]_2$]. This linkage introduces 22 atoms (a maximum of ~2.8 nm) between the ribose oxygens of two ATP molecules. Myosin subfragment 1 (SF_1) or heavy meromyosin (HMM) readily cleave $bis_{22}ATP$ to $bis_{22}ADP$. Upon subsequent addition of excess vanadate ion, both enzymes are rapidly inactivated by formation of a stable vanadate–$bis_{22}ADP$ complex at the active site. By adjustment of the reaction conditions, dimers of SF_1 or HMM, both cross-linked with $bis_{22}ADP$–vanadate, could be prepared. Dimers of SF_1 could be separated from monomers by sucrose gradient centrifugation but not by gel filtration. These observations imply that the average Stokes radius of the dimer approximates that of the monomer, a result predicted only for monomers linked approximately side by side. Conversely, dimers of HMM were separated from HMM monomers by gel filtration, reflecting an increase in their Stokes radii. This increase, however, prevented resolution of HMM dimers from monomers by sucrose gradient centrifugation. These results and the molecular dimensions of $bis_{22}ATP$ suggest that the 3′-(2′)-hydroxyl of ATP is no more than 1.3 nm from the surface of myosin and suggest further in the simplest interpretation that the active site is most likely located near the middle of the heads of myosin. Analytical sedimentation velocity experiments were performed in order to compare the sedimentation coefficient ($s^0_{20,w}$) of the SF_1 dimer formed by cross-linking to values predicted from ellipsoidal models of the dimer. The observed $s^0_{20,w}$ of the dimer was much closer to the range predicted for a side-to-side arrangement of SF_1 monomers than the range predicted for two monomers linked end to end, a result consistent with the active site location suggested above. During the course of these experiments, unmodified SF_1 was used as a control, and its sedimentation behavior was reexamined. We have corroborated the finding that the $s^0_{20,w}$ displayed by SF_1 can be affected to a limited extent by the particular experimental parameters employed during centrifugation [Morel, J. E., & Garrigos, M. (1982) *Biochemistry 21*, 2679–2686]. However, it was demonstrated by equilibrium sedimentation analyses that the variability in $s^0_{20,w}$ could not be explained by shifts in a putative rapid, reversible equilibrium between SF_1 monomer and its dimer [Morel, J. E., & Garrigos, M. (1982) *Biochemistry 21*, 2679–2686].

The mechanism by which energy from the hydrolysis of ATP on the myosin head is converted into the translational movement of myosin and actin filaments remains poorly understood. No large, global conformational changes of the isolated head (SF_1)[1] have thus far been detected upon either the binding or hydrolysis of ATP [for review see Highsmith and Cooke (1983)], and yet it has been estimated that the relative positions of the filaments shift more than 10 nm for each molecule of ATP cleaved (Huxley & Simmons, 1971). In a simple model accounting for these conflicting observations, the heads would act as elongated rigid levers, and a small conformational change derived from nucleotide hydrolysis in a flexible region near one or the other end could produce a large shift in the position of the opposite end (Huxley, 1969; Huxley, 1974). Alternatively, a similar mechanism could be initiated by binding of ATP at some distance from the ends. In this case, a series of conformational effects generated by hydrolysis of the nucleotide would be transferred along the length of the head to a flexible region either at the head–rod junction (hinge) or at the actin binding site(s). These effects might result in a change in the angle of the heads or in rotation of the heads about their long axes.

Quite a different mechanism has been proposed by Harrington (1971, 1979) in which the heads may move very little or not at all. Rather, movement is generated by helix–coil transitions in part of the myosin rod. It might be logically expected that direct regulation of these transitions would occur by ATP hydrolysis in a region close to the head–rod junction. It is clear that knowledge of the position of ATP hydrolysis, even at a low level of resolution, would be useful in modeling the mechanism of force generation. Accordingly, we have initiated a series of investigations whose goal is to locate the site of ATPase activity on the surface of myosin. In a more general sense, this information will be useful in mapping the topography of SF_1 by providing a landmark position against

†Supported by grants from NIH (AM 05195) and MDA. K.B.M. was a postdoctoral fellow of the American Heart Association of Washington. M.J.S. is a recipient of an NIH Research Career Development Award.

[1] Abbreviations: SF_1, chymotryptic subfragment 1 of myosin; HMM, heavy meromyosin; CDI, carbonyldiimidazole; DTNB, 5,5′-dithiobis(2-nitrobenzoic acid); DTE, dithioerythritol; DTCPP, 3,3′-dithiobis[*N*-(5-carboxypentyl)propionamide]; DTSP, 3,3′-dithiobis(succinimido propionate); $bis_{22}ATP$, 3,3′-dithiobis[3′(2′)-*O*-[6-(propionylamino)hexanoyl]adenosine 5′-triphosphate]; $bis_{22}ADP$, 5′-diphosphate derivative of $bis_{22}ATP$; TEA, triethylamine; TEAB, triethylammonium bicarbonate; DMF, dimethylformamide; V_i, orthovanadate; Tris·HCl, tris(hydroxymethyl)aminomethane hydrochloride; TLC, thin-layer chromatography; EDTA, ethylenediaminetetraacetic acid.

0006-2960/86/0425-7640$01.50/0

which other specific sites determined by fluorescence resonance energy transfer [for reviews see Botts et al. (1984) and Morales et al. (1982)] can be compared.

We have used a modification of the approach developed by Valentine and Green (1967) to study antibody structure. These workers synthesized a divalent hapten in which two dinitrophenyl groups were linked with octyldiamine and demonstrated the ability of the reagent to cross-link immunoglobins intermolecularly through their antigen binding sites. Electron microscopy of the cross-linked species demonstrated directly that antigen binding occurs at the tips of the Fab domains. In this report we describe the synthesis of a bisATP analogue in which a bridging group containing 22 atoms (~2.8 nm) links the ribose rings of two ATP molecules. This $bis_{22}ATP$ analogue, in the presence of Mg^{2+} and vanadate ions, can cross-link either SF_1 (intermolecularly) or HMM (both intra- and intermolecularly) via their active sites. Analysis of the sedimentation behavior of cross-linked SF_1 (dimer) suggests that the active site, unlike the binding site of immunoglobulins, is located closer to the center of mass of the heads than to either end.

Materials and Methods

Chemicals. DTSP (Pierce) and imidazole (Aldrich) were recrystallized from acetone/ether and toluene, respectively. 6-Aminohexanoic acid, CDI, DTNB, Li_3ADP, and Na_2ATP were used directly as obtained from Sigma. Sodium orthovanadate was purchased from Fisher Scientific and [2,8-^{3}H]ATP from New England Nuclear. Triethylamine (reagent grade, Baker) was redistilled before use, and TEAB buffers were prepared by bubbling solutions of triethylamine at 0 °C with CO_2 until the desired pH was reached. Dry DMF was stored in the presence of 4-Å molecular sieves after distillation from *p*-toluenesulfonyl chloride. All other chemicals were reagent grade. Buffers were prepared with doubly deionized water.

Protein Preparation. Myosin was isolated from the back and hind leg muscles of rabbits (Wagner & Yount, 1975). Chymotryptic SF_1 was prepared by the method of Weeds and Taylor (1975) and assumed to have a molecular weight of 115 000 with an $\epsilon_{280}^{1\%}$ of 7.5 (Wagner & Weeds, 1977). However, in analyzing and modeling the sedimentation behavior of SF_1, a molecular weight of 107 000 was used to maintain consistency with previous workers [see Morel and Garrigos (1980) and Margossian et al. (1981)]. HMM and papain SF_1 were prepared as described by Margossian and Lowey (1982) and were assumed to have molecular weights of 340 000 ($\epsilon_{280}^{1\%}$ = 6.0) and 133 000 ($\epsilon_{280}^{1\%}$ = 8.3), respectively.

Analytical Procedures. Infrared spectra were obtained with a Beckman AccuLab 1 spectrophotometer, UV–visible spectra with a Cary 14 spectrophotometer, and Raman spectra with a Spectra Physics 164 3-W argon ion laser equipped with a Ramanor HG 2S monochromator and a Spex digital photometer. For $bis_{22}ATP$, total phosphorus (Ames & Dubin, 1960) was determined by the colorimetric method of Rockstein and Herron (1951). The adenine concentration was calculated by assuming an ϵ_{260} of 15 400 M^{-1} cm^{-1}, and the sulfur concentration was measured by reaction of the reduced analogue with DTNB (Ellman, 1959). Reduction was performed by treating 1 mL of 3 mM $bis_{22}ATP$ with DTE (30 mM, 4 °C, 18 h). The reduced nucleotide was lyophilized, redissolved in a minimal amount of methanol, and precipitated by addition of an equal volume of cold acetone (4 °C) saturated with sodium perchlorate. The precipitate was washed 3 times with cold acetone and dried prior to dissolving it in 10 mM sodium phosphate, pH 7.0, for reaction with DTNB. Concentrations of $bis_{22}ATP$ were calculated by assuming an ϵ_{260} of 30 800 M^{-1} cm^{-1}. Magnesium analyses were performed by using a Perkin-Elmer 360 atomic absorption spectrophotometer.

Inactivation Experiments. Solutions of 0.1 M vanadate (ϵ_{260} = 3430 M^{-1} cm^{-1}; Wells & Bagshaw, 1984) were prepared, boiled at pH 10 to destroy polymeric species (Goodno, 1979), and stored at −25 °C. In some experiments inactivated SF_1 was separated from excess nucleotides and V_i by passing the preparations over anion-exchange resin (Dowex 1 × 8) or by gel filtration with Sephadex G-50 (Goodno, 1979). The latter technique was normally used as it gave a much higher recovery of protein (~90% compared to ~50% for anion exchange) at the high protein concentrations used. Specifically, samples were spun at low speed through columns of Sephadex G-50 formed by centrifugation of thick slurries of the resin poured in 5-cm^3 disposable syringes (Penefsky, 1977). Adenosinetriphosphatase (ATPase) assays were performed as described previously (Wells et al., 1979; Wells & Yount, 1980).

HPLC Analyses. Analyses were performed with a C_{18} reverse-phase Spherisorb 5 ODS column (25 × 0.46 cm) from HPLC Technology, Ltd. Two gradient systems (flow rate, 1.5 mL/min) were employed. System I used solvent A (0.1 mM TEAB, pH 6.8) and solvent B [0.1 mM TEAB in 100% ethanol saturated with CO_2(g)] (Mahoney & Yount, 1984). The gradient was 4% solvent B/min. System II used solvent A (same as for system I) and solvent B [0.1 mM TEAB in 100% 2-propanol saturated with CO_2(g)]. The gradient was 1% solvent B/min. Column effluents were monitored with a Beckman Model 165 dual-wavelength detector set at 260 and 280 nm.

Sucrose Gradients. Gradients (40 mL) of 5–20% sucrose dissolved in buffer A (0.1 M KCl, 0.4 mM NaN_3, 50 mM Tris·HCl, pH 8.0) at 4 °C were prepared in Beckman Quick Seal centrifuge tubes. After addition of the samples, tubes were sealed, placed in a precooled Beckman VTi 50 vertical rotor, and spun for 6 h at 49 000 rpm at 4 °C, in a Beckman L8-70 ultracentrifuge.

Sedimentation Velocity Measurements. Sedimentation coefficients were determined on a Beckman Model E ultracentrifuge equipped with schlieren, interference, and scanner optics. Boundary positions were determined from schlieren photographs by using a Nikon microcomparator, except for two experiments in which low concentrations of SF_1 (0.35 mg/mL) required the use of the scanning optical system. All values are reported as the corrected sedimentation coefficient, $s_{20,w}$ [i.e., for water at 20 °C; e.g., Van Holde (1971)]. The specific volume at a given temperature t ($\bar{v}_t$) was calculated for SF_1 from (Svedberg & Pedersen, 1940)

$$\bar{v}_t = \bar{v}_4 - (5 \times 10^{-4})(4 - t)$$

by assuming a value of 0.728 g/cm^3 for $\bar{v}_4$ (Lowey et al., 1969).

Modeling Based on Sedimentation Velocity. The SF_1 monomer was modeled as a prolate ellipsoid and was assumed to have the same structure and hydration in both the free and dimer forms. The axial ratio (a/b) for the hydrated SF_1 monomer was calculated from the ratio of the frictional coefficient for the hydrated monomer (f_m) and the frictional coefficient of a sphere of equivalent mass and hydration ($f_{0,m}$) [e.g., see Van Holde (1971)]. This frictional ratio was determined from the ratio $s_{0,m}/s^0_{20,w}$, where $s_{0,m}$ is the sedimentation coefficient of a sphere of equivalent mass and hydration as the SF_1 monomer at 20 °C and $s^0_{20,w}$ is the sedimentation coefficient of the SF_1 monomer obtained by extrapolation of the measured $s_{20,w}$ to zero SF_1 concentration.

The value for $s_{0,m}$ was obtained by assuming a monomer molecular weight (M_m) of 107 000 and a partial specific

volume (v) of 0.736 cm^3/g with the standard equation:

$$s_{0,m} = (1 - \bar{v}\rho_{20,w})M_m/N_A f_{0,m} \quad (1)$$

where $\rho_{20,w}$ is the density of water at 20 °C and N_A is Avogadro's number. The frictional coefficient of the hydrated sphere ($f_{0,m}$) was obtained from

$$f_{0,m} = [(\bar{v} + \delta\bar{v}_{20,w})/v]^{1/3} f_{min} \quad (2)$$

where δ is the hydration factor (in grams of H_2O/grams of protein), $v_{20,w}$ is the partial specific volume of water at 20 °C, and f_{min} is the frictional coefficient of an unhydrated sphere of equal mass [i.e., $f_{min} = 6\pi\eta_{20,w}(3\bar{v}M_m/4\pi N_A)^{1/3}$]. By use of these expressions, the axial ratio of the monomer was obtained for different hydration levels.

The sedimentation coefficients expected for dimers formed by end-to-end or side-to-side arrangement of monomers with the calculated axial ratios then were estimated for comparison to the value given by extrapolation of the observed sedimentation coefficients to zero dimer concentration. Axial ratios for the dimers were assigned by considering the relative dimensions given by the two extremes of monomer orientations (see Discussion). The ratios were then used to calculate $f_d/f_{0,d}$, where f_d and $f_{0,d}$ correspond to the frictional coefficients of the dimer and of a sphere of mass and hydration equivalent to the dimer, respectively. The molecular weight of the dimer was assumed to be 216 000 (including the weight of cross-linker). Therefore

$$f_{0,d} = f_{0,m}(216000/107000)^{1/3} \quad (3)$$

and an expression analogous to eq 1 was used to calculate the expected sedimentation velocities for dimers corresponding to each hydration value δ.

Sedimentation Equilibrium Analysis. SF_1 preparations were purified by gel filtration through a column of Sephacryl S-400 in buffer A. Fractions containing the major peak were pooled and dialyzed (4 °C) against four changes of a 100-fold volume excess of buffer. SF_1 was used within 1 week of its purification. The sedimentation equilibrium experiments (4 °C) utilized a standard Yphantis cell and interference optics. For each experiment both low-speed (6500 rpm) and high-speed (24 000 rpm; meniscus depletion; Yphantis, 1964) equilibrium patterns were obtained. For analysis of the low-speed fringe patterns, the initial protein concentration (in fringes) was obtained by centrifugation in a synthetic boundary cell (Van Holde, 1967). Fringe positions were read on a Nikon microcomparator and the data processed as described by Van Holde (1967).

Results

Synthesis of DTCPP. To 73 mg (180 μmol) of DTSP (Lomant & Fairbanks, 1976) dissolved in 2.0 mL of DMF was added 71 mg (540 μmol) of 6-aminohexanoic acid in 2.0 mL of H_2O. Additions of 200 μL were made at 1-min intervals with rapid stirring to prevent precipitation of DTSP. Analysis on TLC silica plates (butanol/acetic acid/H_2O in a volume ratio of 5:2:3) showed that all of the *N*-hydroxysuccinimide was released from DTSP within 10 min of mixing. The desired product was isolated either by collecting the excluded volume from a gel filtration column (2.2 × 85.0 cm, Bio-Gel P-2, 200–400 mesh) eluted with 0.1 M TEAB, pH 8.0, or by recrystallization of the dried reaction mixture from a hot aqueous solution (4 mL) (mp 133–135 °C; yield, 72 mg, 62%). Anal. (Galbraith Laboratories) Calcd (Found): C, 49.52 (49.51); H, 7.39 (7.12); N, 6.42 (6.33); S, 14.69 (14.40). Analysis by HPLC (system I) showed a single peak (>90%) well resolved from the elution position of *N*-hydroxysuccinimide. Raman

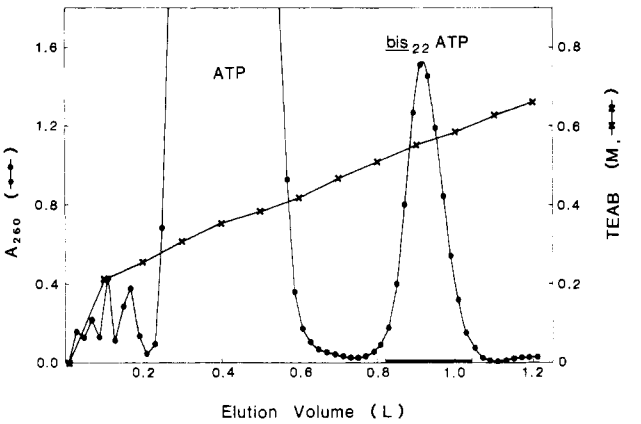

FIGURE 1: Purification of $bis_{22}ATP$ by anion-exchange chromatography. Products from the reaction of ATP with DTCPP were adsorbed onto a column of DEAE-Sephadex and eluted with a gradient of TEAB, pH 7.4. Fractions containing $bis_{22}ATP$ (bar) were combined and lyophilized as described in the text.

absorbance at 500–520 cm^{-1} (dialkyl disulfide stretch), infrared absorbance at 1700–1740 (carboxyl carbonyl stretch), 1630–1650 (amide carbonyl stretch), and 3280–3320 cm^{-1} (amide hydrogen stretch), and slowly decreasing weak UV absorbance from 245 to 320 nm (a distinctive feature of the disulfide moiety) gave further evidence the product was DTCPP.

Synthesis and Purification of $Bis_{22}ATP$. Recrystallized DTCPP (38 mg, 60 μmol) was dried in vacuo and dissolved in 1.0 mL of dry DMF. Solid CDI (195 mg, 1.2 mmol) was added and the mixture stirred for 30 min. Aqueous Na_2H_2-ATP (5.0 mL, 363 mg, 0.6 mmol) was combined with the DMF solution, and after being stirred for 4 h at 21 °C, the mixture was absorbed directly onto a column (1.4 × 22.0 cm) of DEAE-Sephadex. By use of a 1.2-L linear gradient (0.25–0.85 M) of freshly prepared TEAB, pH 7.4, ATP was eluted from the column with 0.27–0.43 M buffer while a second peak of absorbance appeared in the concentration range from 0.52 to 0.60 M (Figure 1). Fractions containing the latter component, subsequently identified as $bis_{22}ATP$, were pooled, diluted 10-fold with cold H_2O, and immediately lyophilized. Dilution was necessary to avoid a small amount of ester hydrolysis that otherwise occurred during freeze-drying. The dry residue was dissolved in 1.5 mL of H_2O, clarified by filtration through cellulose membrane (0.45 μm), and stored at −80 °C (yield, 6 μmol, 10%). The ultraviolet spectrum of the product was nearly identical with that of ATP. Analysis by HPLC (system II) demonstrated the presence of a single major (>95%) component well resolved in the chromatogram from the elution position of ATP. Analyses gave a ratio of 3.80:1.00:0.85 for total phosphate:adenine:sulfur (theory, 4:1:1). On the basis of these results the product was identified as $bis_{22}ATP$ (Figure 2). $Bis_{22}ADP$ was synthesized and purified by an identical procedure and also was shown to be free of contaminants by HPLC. The yield of the bis(diphosphate) analogue (25%) was significantly higher than that obtained for $bis_{22}ATP$.

The possible formation of ATP by ester hydrolysis from $bis_{22}ATP$ (140 μM) was measured at 20 °C in 50 mM Tris·HCl, pH 8.0. Samples from the incubation mixture were analyzed by HPLC at 0, 1, 2, and 3.5 h. No ATP (<1% of $bis_{22}ATP$) was detected, indicating the product was stable under conditions similar to those employed in the cross-linking experiments.

Inactivation of SF_1 and HMM by the Two-Step Procedure. Inactivation of the K^+/EDTA-ATPase activity of SF_1 in the

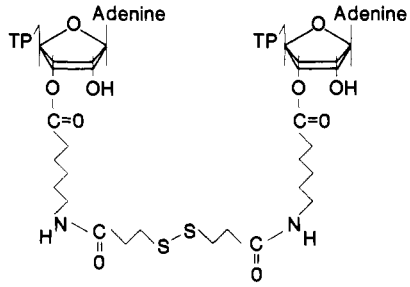

FIGURE 2: Structure of $bis_{22}ATP$. Only the 3′ esters are shown although a mixture of 3′ and 2′ esters is probable.

presence of $bis_{22}ATP$ and V_i in buffer A was performed to assess the ability of both ends of a single reagent molecule to bind simultaneously to separate active sites. Vanadate-promoted inactivation was selected because of the nearly irreversible manner in which ADP is sequestered ("trapped") at the active site of SF_1 when bound in a ternary complex with V_i (Goodno, 1979). It was anticipated that binding at the end opposite one already trapped would be less favorable than the binding of free reagent. To measure attachment at the second end, a two-step inactivation procedure was employed. In this procedure SF_1 was first inactivated with $bis_{22}ATP$ and purified as described under Materials and Methods. This modified inactive SF_1 was combined with fresh, active SF_1 (each species ranged from 20 to 40 μM) and the loss of ATPase activity followed with time after readdition of V_i and Mg^{2+}. Parallel experiments in which ATP was substituted for $bis_{22}ATP$ were run as controls. Several details of the procedure should be noted: (i) Incubation of $bis_{22}ATP$ with Mg^{2+} and SF_1 prior to the first inactivation was required because only the nucleotide diphosphates are trapped as ternary complexes with V_i (Goodno, 1979). Essentially unaltered results were obtained by substituting $bis_{22}ADP$ for $bis_{22}ATP$, and therefore, the conditions of preincubation were considered sufficient to give conversion to the diphosphate analogue. (ii) The V_i-promoted loss of activity was very slow at 4 °C and made the use of higher temperature (20 °C) necessary. (iii) A dilution assay procedure was used in which the concentration of free V_i transferred to the assay solutions from the incubation mixtures had no effect (<5%) on the measured activity. (iv) SF_1 inactivated in a single step with even a small excess of $bis_{22}ATP$ contained no cross-linked species. Therefore, in the case of SF_1, no cross-linking occurs in the initial step of the two-step inactivation procedure, and "modified" SF_1 was assigned the structure SF_1·$bis_{22}ADP$·V_i. By analogy, it was assumed that even a small excess of $bis_{22}ATP$ over active sites in the first inactivation step of HMM was suffiicient to give HMM·2($bis_{22}ADP$·V_i) rather than internal cross-linking between the two active sites of a single HMM molecule. This assumption was later justified by the high yield of intermolecularly cross-linked HMM given by the two-step inactivation procedure (see below). Magnesium ion is trapped with the nucleotide (Wells & Bagshaw, 1984), and therefore, the presence of Mg^{2+} in these complexes is understood.

The results of specific two-step inactivation experiments in which either SF_1 or HMM was used are shown in Figure 3. In the presence of Mg^{2+} and vanadate ion, ADP and $bis_{22}ADP$ (generated by prior enzymatic hydrolysis of $bis_{22}ATP$) both gave rapid and complete inactivation (first inactivation, data not shown). Less than 2% of the starting activity of SF_1 or HMM remained after 10 min of incubation at 20 °C. Cross-linking was evident in the second inactivation step (Figure 3), since the controls displayed only a small decrease in activity (10 ± 5%) while the ATPase activity in the experimental samples decreased to 50% in a period of 3 h. In contrast to the first inactivation with free Mg-$bis_{22}ADP$, activity was lost slowly over a period of several hours at 20 °C during this second incubation.

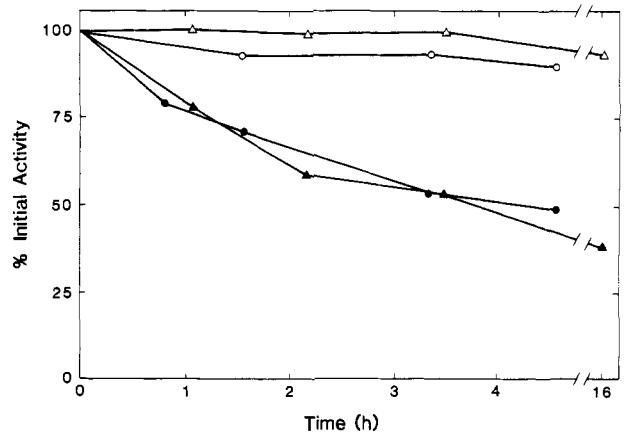

FIGURE 3: Inactivation of SF_1 by SF_1·$bis_{22}ADP$·V_i and HMM by HMM·2($bis_{22}ADP$·V_i), using the two-step procedure. Solutions of SF_1 (60 μM) or HMM (75 μM), $MgCl_2$ (5 mM), and a 2.5-fold excess of either ATP or $bis_{22}ATP$ were incubated at 20 °C for 15 min and assayed for K^+/EDTA-ATPase activity. The activities were measured again after 1 and 10 min of incubation with 1 mM sodium vanadate. Both preparations were completely inactivated by these treatments (data not shown). Excess nucleotide and V_i then were removed from the samples (see Materials and Methods), and the modified preparations were examined for their ability to inactivate, respectively, unmodified SF_1 or HMM. Fresh SF_1 or HMM was added to the solutions. Each sample was assayed prior to readdition of sodium vanadate (ATPase activity at 0 h). Loss of activity then was monitored with time. Final concentrations were 20 μM SF_1·$bis_{22}ATP$·V_i with 34 μM unmodified SF_1 (●) and 30 μM HMM·2($bis_{22}ATP$·V_i) with 35 μM unmodified HMM (▲). Controls were identical but with ADP-trapped protein (SF_1, ○; HMM, △) used in place of protein–$bis_{22}ATP$·V_i. HMM samples were placed on ice after 3.5 h at 20 °C and reassayed after an additional 12.5 h at 4 °C. The fraction of activity remaining, relative to the control, was slightly lower after this treatment but remained constant subsequently (data not shown). Therefore, a 3-h incubation at 20 °C followed by storage of the sample overnight at 4 °C was considered sufficient to complete the cross-linking reaction.

We investigated the inactivation of 10 μM SF_1 with 10, 20, and 30 μM SF_1·$bis_{22}ADP$·V_i at 20 °C in the presence of 1 mM V_i and 2.5 mM $MgCl_2$ and found that the initial rate of inactivation (estimated graphically) was directly proportional to the concentration of SF_1·$bis_{22}ADP$·V_i (apparent second-order rate constant of 10.7 ± 0.02 M^{-1} s^{-1}). This nonsaturating behavior in comparison with ADP alone indicates that the limited accessibility of the unbound end of the trapped $bis_{22}ADP$ was the likely major cause of the apparent poor association constant for the two species (see Discussion). This experiment provided the opportunity to perform a control to show that inactivation in the second step had not resulted simply from reaction of SF_1 with ADP released during the incubation by ester hydrolysis of the trapped $bis_{22}ADP$. In this control, SF_1 at 10 μM and modified SF_1 (but no V_i) at 30 μM were incubated along with the experimental samples described above. No detectable activity loss (<5%) was observed in this sample during the time course of the experiment. After 3 h of incubation at 20 °C, V_i was added. The profile of slow inactivation observed was superimposable with the one found originally for the same concentrations of the two species and demonstrated the absence of free nucleotide.

Sucrose Gradient Centrifugation of Cross-Linked SF_1. The results of the inactivation experiments suggested that about half of the active SF_1 and HMM in the experimental samples had been cross-linked by $bis_{22}ADP$ after 3 h. To observe the

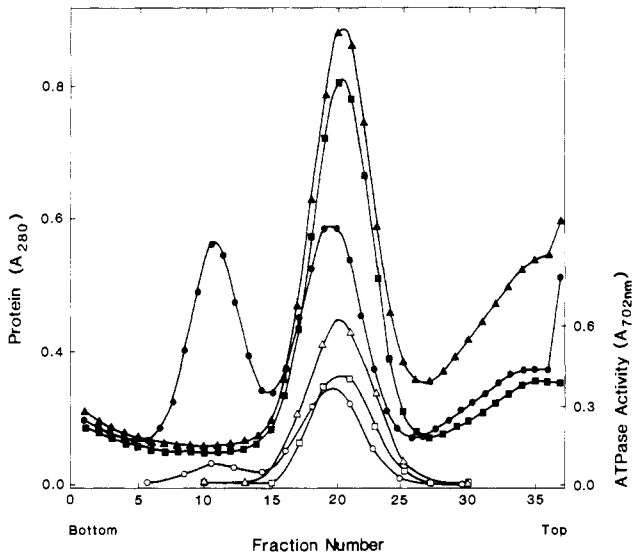

FIGURE 4: Sucrose gradient centrifugation of cross-linked SF_1. The gradients were fractionated and the distributions of protein (A_{280}) (solid symbols) and K^+/EDTA-ATPase activity (A_{702}) (open symbols) measured. Three samples (1.0 mL, 6 mg each) derived from the experiment of Figure 3 were analyzed: (i) SF_1 (34 μM) and SF_1·$bis_{22}ADP$·V_i (20 μM) incubated with 1 mM sodium vanadate for 6 h at 20 °C (●, ○); (ii) the same preparation (1.0 mL) further incubated for 18 h at 4 °C with 30 mM DTE (■, □); and (iii) a control consisting of SF_1 (34 μM) and SF_1·ADP·V_i (20 μM, isolated in the same manner as SF_1·$bis_{22}ADP$·V_i) incubated with 1 mM sodium vanadate for 6 h at 20 °C (▲, △). Background A_{280} is from 0.1 mM sodium vanadate added to prevent possible dissociation of the SF_1 dimer. Later experiments showed this precaution was not necessary. Sedimentation is from right to left.

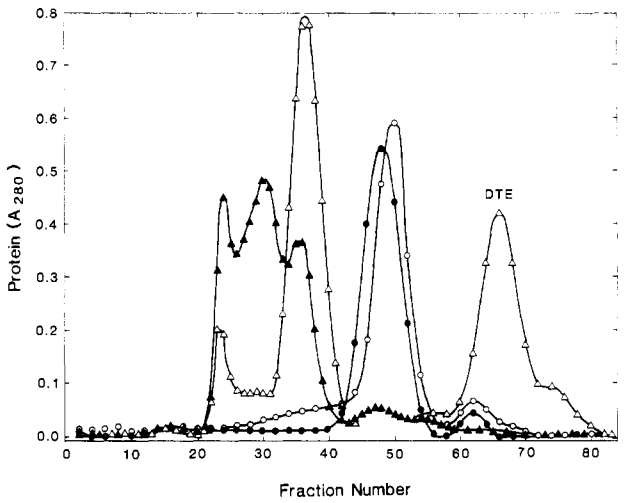

FIGURE 5: Gel filtration of preparations containing either cross-linked SF_1 or cross-linked HMM. Samples of SF_1 (6 mg, ●) or HMM (11 mg, ▲), partially inactivated and cross-linked in the experiment described in Figure 3, were submitted to gel filtration on a column (1.0 × 85 cm) of Sephacryl S-400 (flow rate, 0.1 mL/min). Two separate controls were examined: (△) the same HMM preparation (11 mg) described above incubated with 30 mM DTE (18 h, 4 °C) before gel filtration, and (○) a mixture (6 mg of total protein) of SF_1 and SF_1·ADP·V_i (control from SF_1 experiment of Figure 3). The Mg^{2+} concentration in the HMM fractions was measured by flame spectrophotometry (data not shown). The shapes of the Mg^{2+} profiles were similar to those given by A_{280}. The K^+/EDTA-ATPase activity was assayed through the SF_1 peak region (data not shown). The peak eluting in fractions 60–70 (△) was DTE.

presence of the dimers directly, samples were subjected to centrifugation on sucrose gradients. Results from the SF_1 cross-linking experiment in Figure 3 are shown in Figure 4. The distribution of protein (A_{280}) in the gradients containing cross-linked SF_1 incubated in the presence or absence of 30 mM DTE (18 h, 4 °C) and that in a control (ATP substituted for $bis_{22}ATP$) were compared. Selected fractions from each of the gradients were assayed for ATPase activity. Analysis of the control displayed only a single peak of protein and activity, and this was assumed to be monomeric SF_1. In addition to the monomer, a second protein component was observed further down in the gradient of the cross-linked SF_1. This second component accounted for 44% of the total A_{280} (above background) observed in the gradient and was completely absent from both the sample that had been reduced with DTE and the control (Figure 4). The amount of protein that sedimented at the monomer position (A_{280}) in the reduced sample was equivalent to the sum of the areas under the two peaks observed in the cross-linked sample. It was concluded that the faster protein component was the dimeric complex $2(SF_1$·$V_i)$·$bis_{22}ADP$. The low level of ATPase activity in the dimer peak presumably resulted from dissociation of a small amount of the cross-linked species.

The compound DTSP, employed as a starting material in the synthesis of $bis_{22}ATP$ and $bis_{22}ADP$, has been used as a protein cross-linking reagent. It was found that, in addition to cross-linking, a significant rate of disulfide exchange occurred in some of these experiments (Lomant & Fairbanks, 1976). Accordingly, a separate control was performed to examine the possibility that the dimer was produced by disulfide exchange rather than by trapping at the active site. In this experiment the two-step inactivation procedure produced the usual fraction of dimer (35% of the total A_{280} observed). However, when vanadate (or Mg^{2+}) was not added in the second step, no inactivation occurred and no dimer was found in the sucrose gradients. Since these ions should have no effect on disulfide exchange, it was concluded that this reaction contributed insignificantly to cross-linking.

The stability of cross-linked SF_1 in standard buffer was examined. Repeated sucrose gradient centrifugations demonstrated that the proportion of dimer decreased very slowly ($t_{1/2}$ > 3 weeks for dissociation of dimer) if the cross-linking mixture was kept at 4 °C. Thus, both the cross-linking reagent and the complex containing trapped nucleotide are remarkably stable under these conditions. It was not possible to resolve cross-linked species from monomer in inactivated preparations of HMM by using sucrose gradient centrifugations as only a single broad peak of protein (A_{280}) located at the same position as monomeric HMM was obtained. The presence of cross-linked HMM was suggested in these experiments, however, by a significant change in the shape of the peak upon reduction of the samples with DTE.

Gel Filtration of Cross-Linked HMM. The results of the sucrose gradient centrifugations suggested that an extended conformation of the cross-linked species of HMM may have prevented their separation from HMM monomer on the gradients. Therefore, an attempt was made to separate them on the basis of their size differences. Samples of HMM inactivated with $bis_{22}ATP$ by using the two-step procedure (Figure 3) were submitted to gel filtration on a column of Sephacryl S-400 (Figure 5) at 4 °C. A sample reduced with DTE also was examined as a control. Since Mg^{2+} is trapped at the active site in a complex with ADP and vanadate (Wells & Bagshaw, 1984), the concentrations of Mg^{2+} (not shown) as well as active sites (A_{280}) were determined in the fractions collected during filtration. The shapes of the Mg^{2+} and active site profiles were similar and indicated that a majority (60%) of the HMM had been cross-linked intermolecularly (Figure 5). In the profiles of the reduced sample a significant background of protein containing no trapped Mg^{2+} eluted in fractions 21–31, and

therefore, an accurate estimation of the ratio of Mg^{2+} to active sites for the cross-linked species (eluting in the same region) could only be made by examining the changes in the profiles upon reduction of the sample. Therefore, the concentration profiles (active sites and Mg^{2+}) of the reduced sample were subtracted, fraction by fraction, from those given by unreduced, cross-linked HMM. From these data the molar ratios of Mg^{2+} to active sites gained or lost upon reduction were calculated for each fraction. The ratios (mol of Mg^{2+}/mol of active sites) were 0.76 ± 0.03 and 0.87 ± 0.05 for fractions 26–28 and 29–32, respectively. This result implied that some of the oligomeric species eluting in these fractions were cross-linked through both active sites. In the region of the HMM monomer peak, 0.68 ± 0.11 mol of Mg^{2+}/mol of active sites was recovered after reduction, and therefore, treatment with DTE had little effect on the trapped complex. This observation is consistent with the lack of any effect of DTE upon the ternary complex SF_1·ADP·V_i (Goodno, 1979).

Attempts also were made to separate SF_1 from 2(SF_1·V_i)·bis_{22}ADP by using the same S-400 column. However, the SF_1 monomer nearly coeluted with SF_1 dimer even though HMM and SF_1 could be well resolved (Figure 5). An increase in the specific ATPase activity (data not shown) within the peak region of cross-linked samples that was not found in the profiles of SF_1 chromatographed alone suggested, however, that inactive dimer eluted slightly ahead of the monomer. Subsequent sucrose gradient centrifugation of a portion of the same sample stored at 4 °C during the gel filtration directly demonstrated that 40% of the SF_1 remained in the form of dimer.

One-Step Inactivation and Cross-Linking of SF_1 and HMM. Solutions containing from 35% to 45% 2(SF_1·V_i)·bis_{22}ADP could be produced in either buffer A or buffer B (0.3 M KCl, 0.4 mM NaN_3, 50 mM imidazole, pH 6.8) simply by incubation of a 2.2-fold molar excess of SF_1 (50–70 μM) with Mg-bis_{22}ATP, followed by the addition of sodium vanadate (1 mM). Buffer type had no discernible effect on the yield of cross-linked SF_1. However, when this procedure was applied to HMM at the same active site concentrations, the yields of intermolecularly cross-linked HMM were poor. For both SF_1 and HMM the shape of the ATPase inactivation profiles for this "one-step" procedure appeared to be biphasic (Figure 6). After half of the total loss in ATPase activity occurred within the first 10 min of incubation within V_i while the remainder declined slowly at a rate similar to that observed for the second inactivation of the two-step procedure. Inactivation of SF_1 with excess MgADP and V_i was complete within 10 min. It was concluded that the initial rapid inactivation resulted from trapping of the free reagent at one end while the second inactivation phase was associated with cross-linking. In the case of SF_1, this interpretation was supported further in other experiments by the observation that only a slight excess (1.05-fold) of Mg-bis_{22}ATP over active sites was sufficient to give complete inactivation, but no dimer was formed. It might have been expected from the final levels of inactivation (>50%) observed in the experiment of Figure 6 that the yields of cross-linked species for both SF_1 and HMM would be comparable to those given by the two-step inactivation procedure. This was the case for SF_1. However, while the yield of 2(SF_1·V_i)·bis_{22}ADP was 35%, cross-linked HMM, as measured by gel filtration (see Figure 5), was only 12% of the total A_{280} observed in the column profile. Therefore, internal cross-linking may have occurred between the active sites of a single HMM molecule. To test this possibility, the concentrations of Mg^{2+} in fractions collected during gel filtration were

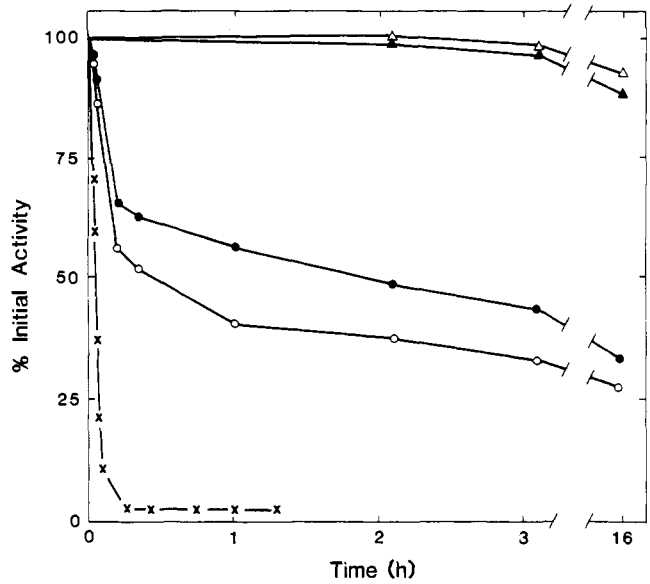

FIGURE 6: Inactivation of SF_1 and HMM by bis_{22}ATP: the one-step procedure. Solutions of SF_1 (48 μM) in buffer B and HMM (65 μM active sites) in buffer A were made 20 and 28 μM in bis_{22}ATP, respectively. After 15 min of preincubation at 20 °C, K^+/EDTA-ATPase assays were performed, and sodium vanadate was added to 1 mM final concentration. Controls received no V_i. Loss of activity with time of incubation (20 °C) was determined (SF_1, ●; SF_1, no V_i added, ▲; HMM, ○; HMM, no V_i added, △). For comparison, an additional inactivation of SF_1 in buffer A and 1 mM V_i was performed with a 2-fold excess of ATP (×) after a similar preincubation.

measured by flame spectrophotometry, and the molar ratio of Mg^{2+} to active sites was calculated for the four fractions containing the HMM monomer peak. The value obtained (0.60 ± 0.02) was greater than could be accounted for by trapping at one end of the bis_{22}ADP, and it was concluded, therefore, that some intramolecular cross-linking had occurred (see Discussion).

Analytical Ultracentrifugation of Cross-Linked SF_1. Solutions containing varying concentrations of cross-linked SF_1 were examined by analytical ultracentrifugation. It was found that, shortly after starting the run, two peaks were resolved by schlieren optics and the change in the position of each then could be monitored independently (see insert, Figure 7). In early experiments, patterns for a particular sample were compared to the protein profiles given by sucrose gradient centrifugation, and the relative amounts of each of the components was shown to be identical. It was concluded that the faster sedimenting peak was 2(SF_1·V_i)·bis_{22}ADP and the slower sedimenting peak was SF_1 monomer. The homogeneity of both species was suggested by the continued symmetry of the peaks throughout the centrifugation.

It has been shown by Morel and Garrigos (1982) that $s_{20,w}$ increases to a limiting, maximum value as the rotor speed is raised. It was concluded that, up to this limit, the sedimentation velocity of SF_1 is positively correlated to hydrostatic pressure, and therefore, these authors recommended that sedimentation velocities be calculated for SF_1 from data obtained in a narrow range (<0.18 cm) of distances (r) from the center of rotation and as close to the meniscus of the solution column as possible (<0.28 cm). However, resolution of monomer from dimer was required for measurement of their individual sedimentation velocities, and it was not possible to measure changes in boundary positions (Δr) near the meniscus. Nevertheless, no systematic deviation in the linearity of the relationship between r and time was found in the range of distances examined (Δr < 0.3 cm, 6.2 cm < r < 6.7 cm,

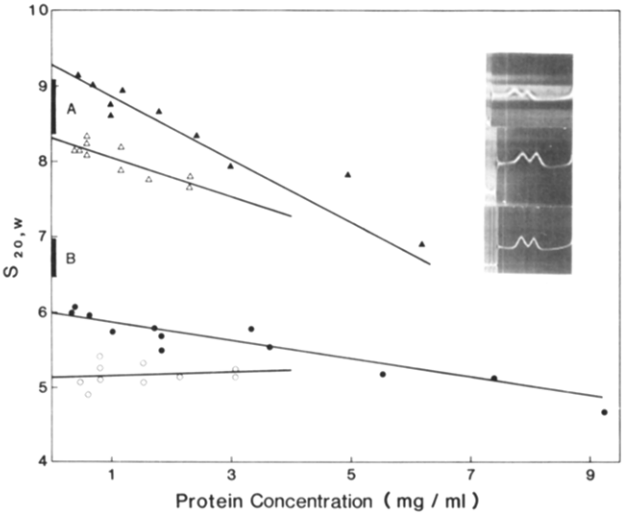

FIGURE 7: Sedimentation coefficient vs. initial concentrations of SF_1 and $2(SF_1{\cdot}V_i){\cdot}bis_{22}ADP$. Mixtures of the two species were subjected to centrifugation under two separate sets of conditions: set I [SF_1, ●; $2(SF{\cdot}V_i){\cdot}bis_{22}ADP$, ▲] in buffer A, 56 000 rpm, temperatures between 5.5 and 9.5 °C, and set II [SF_1, ○; $2(SF_1{\cdot}V_i){\cdot}bis_{22}ADP$, △] in buffer B, 40 000 rpm, 20.0 °C. Initial concentrations were calculated on the basis of the total protein concentration (A_{280}) and the proportion of each species present. No correction was made for radial dilution. Included are two values of $s_{20,w}$ (~6.0) obtained for SF_1 alone at low concentrations (0.35 mg/mL) by using a scanning optical system (A_{280}). The fits shown were determined by linear regression. Vertical bars on the ordinate axis represent a range of values for $s^0_{20,w}$ estimated for dimers of different hydrations (0.4–1.37 g of H_2O/g of protein) formed by either side-to-side (A, top) or end-to-end (B, bottom) cross-linking of SF_1 modeled as a prolate ellipsoid (see Discussion). The inset shows a representative set of schlieren photographs for three samples differing in total protein concentration. Direction of sedimentation is from left to right. The concentrations of monomer and dimer were calculated from the total protein concentration and the fractional amount contributed by each species. Top plate: monomer, 0.76 mg/mL; dimer, 0.58 mg/mL; 40 000 rpm, 20 °C, buffer B. Middle plate: monomer, 1.53 mg/mL; dimer, 1.15 mg/mL; other conditions, same as top plate. Bottom plate: monomer, 3.61 mg/mL; dimer, 2.41 mg/mL; 56 000 rpm, 9.5 °C, buffer A.

meniscus at 6.0 cm). Moreover, the expected minimum value of $s_{20,w}$ was obtained under conditions designed specifically to favor the slower form of SF_1 (see set II conditions, legend of Figure 7), and therefore, pressure effects were not overriding.

Sedimentation coefficients were calculated from schlieren data and the corrected values ($s_{20,w}$) plotted as a function of protein concentration for both monomer and dimer (Figure 7). The initial concentrations of dimer and monomer were determined by multiplying the total measured SF_1 concentration with the properties of each calculated from integration of the schlieren peaks. It was found that the position of an individual peak was measurable only for species whose initial concentration was greater than 0.4 mg/mL. Since it had been reported that the apparent sedimentation velocity of SF_1 depends upon the particular conditions employed to examine it (Morel & Garrigos, 1982), two sets of experimental parameters were selected to favor either SF_1 with a relatively high sedimentation velocity (set I: cross-linking and centrifugation performed in buffer A; centrifugation at 56 000 rpm, 5.5–9.5 °C) or SF_1 of lower sedimentation velocity (set II: cross-linking and centrifugation in buffer B; centrifugation at 40 000 rpm, 20 °C). All solutions examined contained 1 mM sodium vanadate and 5.0 mM $MgCl_2$ in addition to trapped $bis_{22}ADP$. Although the monomer in these experiments was comprised of a mixture of free SF_1 and SF_1 containing trapped Mg-$bis_{22}ADP$, no apparent heterogeneity of this species was observed (see insert, Figure 7). At concentrations less than 3

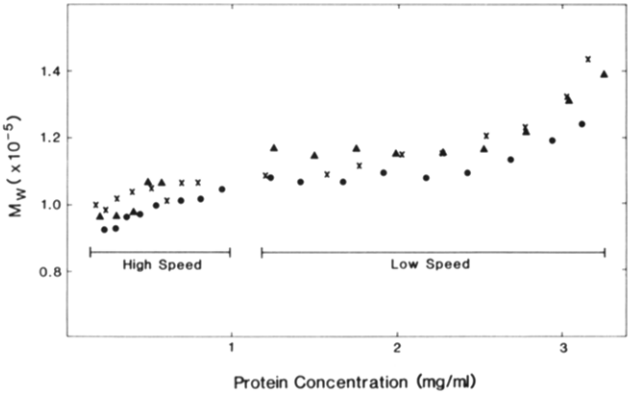

FIGURE 8: Weight-average molecular weight as a function of protein concentration in the sedimentation equilibrium cell. SF_1, in three separate buffer systems, was examined first by low-speed (6500 rpm) and then high-speed (24 000 rpm) sedimentation equilibrium at 4 °C by using interference optics. Initial loading concentrations were 2.0 mg/mL. $SF_1(A_1)$ and $SF_1(A_2)$ were not separated, but the preparation was purified by gel filtration prior to dialysis against buffer A (●), buffer B (×), or buffer C (▲). See text for details.

mg/mL the conditions of set II gave lower values of $s_{20,w}$ for both SF_1 monomer and dimer than did the conditions of set I. Extrapolation to zero concentration gave the following values for $s^0_{20,w}$: set I, 6.0 for monomer and 9.3 for dimer; set II, 5.1 for monomer and 8.3 for dimer (Figure 7). The standard deviation of these measurements was 0.14 S.

Sedimentation Equilibrium. The possibility that a weak, reversible dimerization of SF_1 was responsible for the higher $s^0_{20,w}$ observed under the set I parameters was examined. A standard SF_1 preparation was purified further by gel filtration at 4 °C and then extensively dialyzed against buffer A, buffer B, or buffer C (20 mM KCl, 5 mM $MgCl_2$, 2 mM ADP, 2 mM DTE, 50 mM imidazole, pH 7.5). The three samples were subjected to centrifugation together in the same rotor cell. The distributions of protein at equilibrium were determined first at low speed and then at high speed (i.e., after depletion of the meniscus) without stopping the run. From these data, weight-average molecular weights (M_w's) were calculated as a function of protein concentration for each distribution. The results are presented in Figure 8. It has been reported by Morel and Garrigos (1982) that SF_1 displays a molecular weight of 215 000 when examined by equilibrium sedimentation analysis in buffer C. However, in our hands, no significant difference in the M_w profile could be detected for the different buffer conditions. Preparations of SF_1 not purified by gel filtration also were examined by low-speed sedimentation equilibrium. Results nearly superimposable with those presented in Figure 8 were obtained for protein concentrations below 2 mg/mL. Above this concentration, sharp deviations of M_w toward higher values were observed for all three samples. Furthermore, a small amount of protein (<-10%) was observed in the excluded volume during gel filtration of SF_1. Therefore, these higher molecular weight components, possibly undigested myosin or myosin tails, may account for the upward curvature seen in the M_w profiles for the sedimentation equilibrium analysis.

A somewhat lower average M_w (102 000) was given by the high-speed method (concentrations of SF_1 < 1 mg/mL) when compared to those given by the low-speed procedure (112 000). However, it is known that standard preparations of SF_1 contain two isoenzymes of slightly differing molecular weight, i.e., about 1.5 mol of $SF_1(A_1)$, M_w 110 000, for every mole of $SF_1(A_2)$, M_w 100 000 [see Margossian et al. (1981)]. Such a mixture would be expected to give a decrease in M_w at low

protein concentrations. Moreover, even after separation of the isoenzymes, other workers have found a similar, minor decrease in M_w at low concentrations of both $SF_1(A_1)$ and $SF_1(A_2)$ (Margossian et al., 1981). Nevertheless, the central feature of importance in these analytical experiments was the lack of buffer effects on the M_w profile. To confirm this observation, further sedimentation analyses (by meniscus depletion) were performed by using SF_1 not purified by gel filtration. In these experiments, data were obtained for chymotryptic SF_1 in both buffer A and buffer B, as well as for papain SF_1 in buffer A. All three samples were centrifuged together in a standard Yphantis cell. The plots of ln c vs r^2 were nearly linear but again showed some slight curvature in the region corresponding to low concentration (below ~0.1 mg/mL) where uncertainty in the measured fringe displacement was high. From the combined data of five separate experiments, the molecular weights of chymotryptic SF_1 in buffer A, chymotryptic SF_1 in buffer B, and papain SF_1 in buffer A (calculated for the concentration range of 0.15–0.85 mg/mL) were 100 500 ± 7300, 99 400 ± 5600, and 129 000 ± 6900, respectively.

Discussion

A bisATP reagent has been synthesized for the purpose of cross-linking SF_1 or HMM via their active sites. The ultimate goal has been to determine the location of the active site on the surface of the myosin head. Development of this new approach required an analogue sufficient in length to allow binding at each of its ends simultaneously. Furthermore, in order to separate cross-linked species, it was necessary to use a compound that could be trapped in the active site with vanadate ion in a manner analogous to that of ADP (Goodno, 1979).

Several early attempts to produce such a reagent were unsuccessful. In one case, a promising bisATP derivative was isolated in good yield (>60%) after reaction of adipic dihydrazide with purified periodate-oxidized ATP (roATP). This reaction, modeled on that used by Lamed and Oplatka (1974) to prepare ATP affinity columns, yields a product in which the ribose of ATP is replaced by a modified morpholine ring (Hansske et al., 1974). The dihydrazide adduct was found to be stable in aqueous solutions (pH 8.0) and was hydrolyzed by SF_1, under saturating substrate concentrations, even more rapidly than ATP itself. However, addition of V_i (1 mM) and 5 mM Mg^{2+} gave no inactivation, and this cross-linking approach was abandoned. In fact, even roATP (roADP) itself was not trapped by addition of V_i and Mg^{2+}, and it was felt that analogues which contained intact ribose rings were necessary. Hiratsuka (1984) and our own unpublished observations (R. Mahmood and R. G. Yount) have shown that V_i with Mg^{2+} will stabilize the binding of a variety of ADP analogues esterified at ribose 3′(2′)-hydroxyls to myosin. The usual synthetic procedure for ATP derivatives of this type involves formation of an acid–imidazolate in dry DMF followed by addition of excess aqueous ATP (Gottihk et al., 1969). However, several attempts to synthesize a bisATP or bisADP reagent by this procedure from recrystallized sebacic acid or 3,3′-dithiobis(propionic acid), both designed to give an eight-atom cross-link, were unsuccessful. It was assumed that repulsive interactions of the highly charged ATP at the ends of these bridging compounds had destabilized the transition states required for the formation of the desired products. It was necessary to synthesize a longer DMF-soluble dicarboxylic acid. Reaction of 2 mol of 6-aminohexanoic acid with DTSP as described here provided the desired bridging compound, DTCPP, in high yield and purity. In contrast to the shorter bridging compounds discussed above, esterification of DTCPP with ATP was achieved in the expected yield (30% coupling at each end to give ~10% yield of $bis_{22}ATP$), and therefore, the coupling reactions at each end occur independently from one another. The large negative charge of $bis_{22}ATP$ allowed for its rapid purification from the starting materials by anion-exchange chromatography. $Bis_{22}ATP$ isolated in this manner was pure by HPLC and contained adenine, phosphate, and sulfur in the predicted molar ratios. While we have used reduction of the disulfide group in experimental controls, this procedure can also provide a thiol at the end of a long side arm to be used to prepare other ATP analogues.

Inactivation and Cross-Linking. Vanadate-mediated trapping of $bis_{22}ADP$ (generated enzymatically) was used to cross-link both SF_1 and HMM. It is known that ADP is required for trapping with V_i at the active site of SF_1. Excess ATP inhibits the rate of V_i inactivation (Goodno, 1979), presumably by sterically blocking the position of V_i binding. Therefore, preincubation of $bis_{22}ATP$ with SF_1 was required to convert the analogue to the bis(diphosphate) derivative. Successful trapping was obtained by this procedure and occurred at a rate similar to that given by the same concentrations of enzymatically hydrolyzed ATP. This result demonstrates that $bis_{22}ATP$ is a substrate for myosin.

The ability of inactive SF_1, containing trapped $bis_{22}ADP$, to inactivate unmodified SF_1 provided the initial indirect evidence for cross-linking. This secondary inactivation was shown to be specific for the active site by its requirement for V_i and Mg^{2+} and was not the result of release of ADP by possible ester hydrolysis from the bound reagent. The initial rate of vanadate-mediated inactivation by trapping of free $bis_{22}ADP$ (2-fold excess over active sites) was indistinguishable from that given by the same concentration of ADP. However, the secondary inactivation to give cross-linked species was much slower (Figures 3 and 5). Thus, esterification of ATP at the hydroxyls of the ribose ring in $bis_{22}ATP$ appeared to have little or no effect on trapping of the free compound. However, if one end of the bis analogue was already attached at an active site, binding of the other end was greatly inhibited. A poor association of $SF_1{\cdot}V_i{\cdot}bis_{22}ADP$ with SF_1 could account for this result. Accordingly, the rate of inactivation of unmodified SF_1 (10 μM) increased linearly with increasing $bis_{22}ADP$-modified SF_1 up to 30 μM, the highest concentration examined. This can be contrasted with the observation that stoichiometric amounts of ADP ($K_a \sim 10^6$ M^{-1}) gave the maximal rate of vanadate-mediated inactivation of SF_1 at 20 μM sites (Goodno, 1979). A relatively low affinity of $SF_1{\cdot}bis_{22}ADP{\cdot}V_i$ for $SF_1{\cdot}V_i$ would explain the low rate of secondary inactivation if conversion to the inactivated species was preceded by equilibrium binding of $SF_1{\cdot}V_i$ with $SF_1{\cdot}bis_{22}ADP{\cdot}V_i$. In this case the apparent initial rate of secondary inactivation is $k_c K_a[SF_1{\cdot}bis_{22}ADP{\cdot}V_i][SF_1{\cdot}V_i]$, where K_a is the association constant for the $SF_1{\cdot}bis_{22}ADP{\cdot}2V_i{\cdot}SF_1$ complex, k_c is the rate of isomerization of this complex to the trapped (cross-linked) complex, and vanadate [K_d = 320 μM, Wells and Bagshaw (1984)] at 1 mM is assumed to be saturating for SF_1. A value for K_a of ~10^3 M^{-1} was calculated from the apparent rate constant observed for the secondary inactivation (10.5 M^{-1} s^{-1}) and the value of k_c (0.01 s^{-1}) estimated by Goodno (1979). This analysis assumes that juxtaposition of the two SF_1 monomers has little effect on k_c.

HMM modified in both active sites by trapping 2 mol of $bis_{22}ADP$ was capable of inactivating unmodified HMM with a rate comparable to $SF_1{\cdot}bis_{22}ADP{\cdot}V_i$ inactivation of SF_1 at similar active site concentrations (Figure 5). Thus, attachment of the heads to the myosin tail had no apparent effect on the

rate of intermolecular cross-linking in the two-step inactivation procedure. This would be an unlikely result if the active site were located near the head–rod junction.

The rate profiles for inactivation resulting from incubation of a 2.2-fold excess of active sites over $bis_{22}ADP$ were similar for SF_1 and HMM. In this one-step procedure, the inactivation kinetics were biphasic. The first phase was rapid and appeared to be dominated by trapping of free $bis_{22}ADP$ at one end while the secondary, slow phase was associated with cross-linking. For HMM, however, a limiting level of inactivation was approached at a slightly faster rate. Direct examination by chromatographic separation showed no dependence of the yield of cross-linked SF_1 on the method of inactivation. However, a dramatic increase ($\sim$5-fold) in intermolecular cross-linked species of HMM was obtained by using the two-step procedure. It appeared from these results that by using the one-step method the two heads of HMM can be cross-linked to one another. An estimate of the minimum amount of intramolecular cross-linking can be made by considering the ratio of Mg^{2+} to active sites found for HMM monomer in the experiment of Figure 6. The yield of intermolecular cross-linked HMM dimer (12%) implies that 29 μM HMM (58 μM active sites) of the 33 μM total in solution remained as monomer. A minimum of 2 μM $bis_{22}ADP$ is required to give 4 μM intermolecularly cross-linked HMM (one cross-bridge for each HMM dimer), and a maximum of 26 μM $bis_{22}ADP$ then would be available to trap with V_i and Mg^{2+} on the HMM eluting in the position of monomer. Therefore, if no intramolecular cross-linking could occur, a ratio of Mg^{2+} to active sites of 0.45 (26/58) in the fractions corresponding to monomer would be expected. The observed value (0.60 $\pm$ 0.02) implies that a minimum of one-third of the trapped reagent has cross-linked the two active sites of a single HMM molecule.

Considering the dependency of intermolecular cross-linking on the method of inactivation, the similarity in the single-step inactivation rate profiles for SF_1 and HMM may seem unexpected. A preference for intramolecular cross-linking would imply a more rapid rate of inactivation for this reaction compared to that given by intermolecular cross-linking. However, the formation of some HMM modified at both of its active sites, a maximum of $(0.45)^2$ or $\sim$20% of the total, during the initial phase of the inactivation would be expected under the conditions used (1.1-fold excess HMM over $bis_{22}ADP$). Subsequent intermolecular cross-linking then would give rise to the observed slow loss of activity in the latter stages of the incubation and may be responsible for the small amount of cross-linked HMM dimer observed in this sample.

Of central importance in these experiments was the direct demonstration of SF_1 dimers formed by cross-linking through the active sites. Dimers of SF_1 could not be separated from monomers on a column of Sephacryl S-400 that would well resolve HMM from SF_1. This result indicated that an insignificant change in the radius of gyration had occurred upon cross-linking, and therefore, it was probable that little change occurred in the frictional coefficient as well. Sucrose gradient centrifugation, a technique in which the velocity of sedimentation is proportional to the ratio of particle weight to the frictional coefficient, provided the expected separation. These results are consistent with a model for the dimer in which the cross-linked SF_1 monomers are highly overlapped. Addition of DTE to the cross-linking mixture eliminated the dimer and demonstrated the presence of a disulfide bond in the linkage between monomers. Because no dimer was formed without addition of V_i and Mg^{2+} in the second step of the two-step inactivation procedure, disulfide exchange does not contribute significantly to dimer formation. Inactivation in the second step and its requirement for these ions, considered together with the direct observation of a separable species composed of SF_1 but of greater mass, represent strong evidence for the formation of a stable dimer of SF_1 by active site cross-linking with $bis_{22}ADP$.

From a Corey–Pauling–Koltun (CPK) model of $bis_{22}ADP$, a distance of $\sim$2.6 nm was measured between carbonyls for the most extended conformation of the cross-bridge. If the region of the protein surrounding the binding site in its trapped conformation were flat, the depth at the 3′-hydroxyl of the nucleotide could be no more than $\sim$1.3 nm from the protein surface. This conclusion coupled with the fact that the cross-bridge must extend out of the trapped sites makes less likely a model in which trapping occurs concurrently with the folding of a large portion of the primary structure over the active site.

Analytical Sedimentation. The sedimentation coefficients of SF_1 and $2(SF_1 \cdot V_i) \cdot bis_{22}ADP$ were analyzed as a basis to determine the relative arrangement of SF_1 monomers in the dimer. Because the experiments were performed with solutions containing both monomer and dimer (Figure 7), SF_1 itself served as an internal standard in these experiments. For this reason, a potential complication had to be considered. It has been reported (Morel & Garrigos, 1982) that the conditions employed during ultracentrifugation can affect the value of $s_{20,w}$ observed for SF_1. These authors postulated that SF_1 exists in equilibrium with its dimer ($dimer_{eq}$) and factors such as temperature, ionic strength, pH, and rotor speed influence this equilibrium. The conclusion was made that conditions giving higher values of the apparent sedimentation coefficient ($s^{app}_{20,w}$) shifted the equilibrium in favor of $dimer_{eq}$. By extrapolation of the sedimentation data to zero concentration, the monomer and $dimer_{eq}$ were assigned values for $s^{app,0}_{20,w}$ of 5.05 $\pm$ 0.05 and 6.05 $\pm$ 0.05, respectively. The relatively small increase in $s^{app,0}_{20,w}$ was accounted for by assuming an end-to-end arrangement of the monomers to form $dimer_{eq}$. Thus, the asymmetry of $dimer_{eq}$ could account for its low sedimentation velocity. This interpretation seems unlikely, however, since an axial ratio of 1:12 for $dimer_{eq}$ (modeled as a prolate ellipsoid) was required to fit the data, whereas the derivation was initiated by modeling the monomer as a prolate ellipsoid with an axial ratio of 1:4. Perhaps the most convincing evidence for the existence of the $dimer_{eq}$ was the molecular weight (215000) calculated for SF_1 from an equilibrium sedimentation experiment performed under conditions specifically selected to favor $dimer_{eq}$ formation (Morel & Garrigos, 1982).

In order to avoid the potential complications presented by the presence of $dimer_{eq}$, we performed sedimentation velocity experiments under a set of conditions (set II) that were expected to favor monomers as well as under those (set I) normally employed in studies of SF_1 which, it was suggested, favor the formation of the $dimer_{eq}$ (Morel & Garrigos, 1982). The latter conclusion originated from a consideration of the values of $s_{20,w}$ ($\sim$5.8) usually observed for SF_1 [see Lowey et al. (1969)] under conditions similar to those of set I. Our results agree well with this value (set I, Figure 8) and support the measurements performed by others.

The sedimentation experiments we have presented corroborate, in part, those of Morel and Garrigos (1982). Under the conditions of set II, extrapolation to zero SF_1 concentration gave a significantly lower value for $s^0_{20,w}$ (5.1) compared to that found by using the set I conditions (6.0). From the agreement of these values with those predicted for pure SF_1 monomer and the putative $dimer_{eq}$ (Morel & Garrigos, 1982), it might

be concluded that each species predominates, respectively, under the conditions selected to favor them. In order to test this theory, SF_1 was examined by sedimentation equilibrium in the buffers of sets I and II, as well as in a buffer of identical composition to the one reported by Morel and Garrigos (1982) to have given the calculated molecular weight of 215 000 for SF_1. Comparison of the behavior of SF_1 in these samples was simplified by submitting them to centrifugation simultaneously in the same cell and utilizing both low- and high-speed (meniscus-depletion) methods. As the results of Figure 8 show, we were unable to confirm any significant dependency of M_w on either the different buffer conditions or the concentration of SF_1 up to ~2.5 mg/mL. In addition, repeated individual analyses by the meniscus-depletion method (concentrations less than 1 mg/mL) failed to show any buffer-dependent change in the molecular weight of SF_1 whereas the expected difference between the molecular weights of chymotryptic SF_1 and papain SF_1 (included for comparison) was observed. However, a significant difference in the $s_{20,w}$ of SF_1 was observed in this concentration range for the two sets of conditions.

The sedimentation coefficient of cross-linked SF_1, obtained by extrapolation to zero concentration, displayed a sensitivity to the conditions of centrifugation similar in magnitude and direction to that of SF_1 alone. Set I conditions gave a higher extrapolated value for $s^0_{20,w}$ (9.3) than was found when the conditions of set II were used (8.3) (see Figure 7). It appears, therefore, that the factor(s) affecting the increased $s^0_{20,w}$ for the monomer also can influence the dimer. On the basis of this assumption and the sedimentation equilibrium experiments, it must be concluded that shifts in a rapid, reversible equilibrium between SF_1 monomer and $dimer_{eq}$ cannot be the explanation for changes in the value of $s^0_{20,w}$ of SF_1 observed in this study. If this equilibrium were to exist, then by analogy, changes in $s_{20,w}$ observed for the cross-linked complex of SF_1 ought also to be explained by a similar reversible reaction in which monomer (or cross-linked dimer) can combine with $2(SF_1 \cdot V_i) \cdot bis_{22}ADP$ to form a trimer (or tetramer). This equilibrium would be shifted in favor of the trimer (or tetramer) under the conditions of set I to give the higher $s^0_{20,w}$ observed. This assumption implies further that polymerization of $2(SF_1 \cdot V_i) \cdot bis_{22}ADP$ should occur to some extent under these circumstances. Even setting aside this complication, it is clear that such an equilibrium of SF_1 with $2(SF_1 \cdot V_i) \cdot bis_{22}ADP$ would necessarily prevent resolution of monomer from dimer by the methods used here. In fact, resolution was obtained both by sucrose gradient centrifugation (Figure 4) and by moving-boundary centrifugation (cf. insert, Figure 7, bottom plate, set I conditions) under conditions that should have given oligomeric species (assuming that rapid equilibrium exists).[2] Nevertheless, in order to avoid this problem, the modeling calculations (described below) were performed by substituting sedimentation velocity values calculated from data gathered for the monomer-promoting conditions of set II. It remains to be determined why the sedimentation velocity of SF_1 is affected significantly by changes in buffer conditions. However, it appears that the variability of $s^0_{20,w}$ is a property of the SF_1 monomer presumably related to changes in hydration or frictional coefficient. The physiological significance (if any) associated with this phenomenon has yet to be established, but it is apparently not related to ADP binding since mixtures of monomer species (with and without trapped nucleotide) displayed homogeneous behavior.

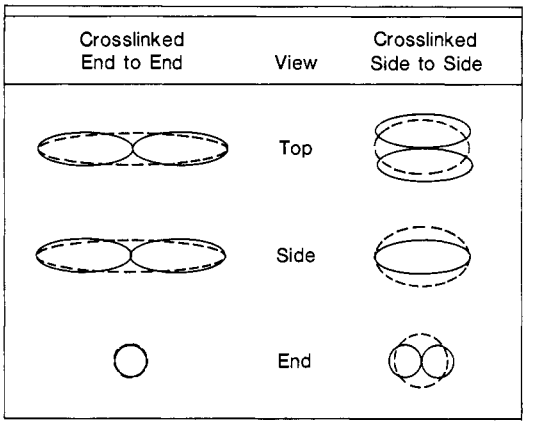

FIGURE 9: Schematic views of prolate ellipsoids ($a/b = 3$) cross-linked end to end or side to side. The dashed lines represent the shapes of the dimers used as models for each of the two extremes in monomer arrangement.

The sedimentation velocity data of cross-linked SF_1 suggest that the binding site for ATP hydrolysis is not located at either of the ends of SF_1.[3] This conclusion assumes that the structure of $2(SF_1 \cdot V_i) \cdot bis_{22}ADP$ can be approximated by a prolate ellipsoid of revolution. If the axial ratio of such an ellipsoid is known, then its sedimentation velocity can be predicted. We have assigned axial ratios on the basis of two orientations of monomers in the dimer, side to side or end to end. These extremes would arise if the active site were located either in the middle or at the ends of SF_1, respectively. In order to assign axial ratios for each type of orientation, SF_1 also was modeled as a prolate ellipsoid and its axial ratio calculated from the extrapolated value (5.1) of $s_{20,w}$. These ratios will depend upon the level of hydration of SF_1, and we have assumed that the hydration of $2(SF_1 \cdot V_i) \cdot bis_{22}ADP$ is the same as that of SF_1. Because the level of hydration associated with SF_1 is unknown, we performed a set of modeling calculations for several different values of hydration. A particular hydration value was assumed, the sedimentation velocity ($s_{0,m}$) for a sphere of mass and hydration equivalent to those of SF_1 was calculated (eq 1 and 2), and the ratio of the frictional coefficients for SF_1 (f_m) and the sphere ($f_{0,m}$) was determined from $f_m/f_{0,m} = s_{0,m}/s_m$. Since the functional dependence of this ratio on the axial ratio (a/b) of a prolate ellipsoid is known (Van Holde, 1971), a value for a/b could be found that satisfied the relationship to any desired approximation (in this case, within 0.2%). By use of this procedure, the axial ratio for the SF_1 monomer was calculated for different levels of

[2] While this report was in preparation, new evidence for $dimer_{eq}$ formed from papain SF_1 was published (Bachouchi et al., 1985). Electron micrographs of SF_1 prepared by a freeze–fracture technique were presented, showing structures identified as $dimer_{eq}$. The micrographs, however, were prepared from high protein concentrations (7–10 mg/mL) in solutions containing 30% glycerol. Although the 30% glycerol was stated to have no effect on the sedimentation behavior of SF_1, these latter measurements were made at protein concentrations below 1 mg/mL. Regardless of the explanation for the dimeric structures observed by Bachouchi et al. (1985), it is clear the SF_1 dimers observed here resulted from cross-linking by $bis_{22}ADP$ and not from self-association.

[3] Our results do not rule out the possibility that $bis_{22}ADP$ binding at either end of two SF_1 molecules could promote the parallel self-association of the heads. Such a dimer could behave hydrodynamically as if it were cross-linked in the middle. However, since the completion of this work, Sutoh et al. (1986) have shown by electron microscopic analysis of myosin–avidin complexes formed after labeling myosin's active site with a photolabile ATP–biotin photoprobe that the active site was located approximately two-thirds of the distance from the hinge to the end of the head. Likewise, our recent electron microscopic observations of HMM cross-linked both intra- and intermolecularly by $bis_{22}ADP$ (K. Munson, S. Lowey, and R. Yount, unpublished results) place the active site in the thick part of the head, again about two-thirds of the distance from the hinge to the end of the heads.

hydration. The range of hydration values chosen was from 0.4 (where $a/b = 6.50$) to 1.37 g of H_2O/g of protein (where $a/b = 2.75$). This range of hydration values was selected to include the relatively high value (1.37) suggested by Garrigos et al. (1983) and a value representative of a reasonable lower limit (0.4) for SF_1 [cf. Yang and Wu (1977)]. It then was possible to assign axial ratios for the two extremes of monomer orientations in the dimer. The end-to-end arrangements of monomers were assumed to give an axial ratio for the dimer 2-fold greater than that of the monomer. This assumption was made because the shorter axial dimension would be equivalent to that of the monomer (see Figure 9). For side-to-side arrangements of monomers, however, there are three unequal dimensions in the dimer, and therefore, an average of the two closest dimensions in numerical value was taken as one of the axial dimensions of the ellipsoid (Figure 9). For instance, a side-to-side arrangement of prolate ellipsoids with axial ratios of 6.50 would have dimensional ratios of 6.50:2.00:1.00. This structure was modeled as a prolate ellipsoid with axial ratio 6.5/1.5 or 4.33. A similar analysis was used to estimate axial ratios for the other dimers formed from side-to-side cross-linking. By use of these axial ratios to calculate $f_d/f_{0,d}$ for each dimer, the expected sedimentation coefficient was estimated from eq 1 since the frictional coefficient ($f_{0,d}$) for a sphere of mass and hydration equal to that of the dimer can be calculated from eq 3. The range of sedimentation velocities for each type of arrangement is shown on the ordinate axis of Figure 7, where A signifies side-to-side configurations and B signifies end-to-end configurations. The extrapolated sedimentation coefficient ($s^0_{20,w}$) of the dimer (8.3) is nearly within the range of values predicted for the side-to-side arrangement of monomers but is more than 1.2 svedbergs from those predicted for monomers cross-linked via their ends. Thus, even in this crude approximation, it can be concluded that the monomers are overlapped extensively in the dimer and that the ATP binding site is likely not located at either of the extreme ends of the myosin head but is probably close to its center of mass.

ACKNOWLEDGMENTS

We thank Jean Grammer and Jana Patton for technical assistance, Sue Sheets for typing the manuscript, and Dr. S. Gurusiddaiah for performing the analytical ultracentrifuge runs.

Registry No. V_i, 14333-18-7; DTCPP, 104693-49-4; DTSP, 57757-57-0; Na_2H_2ATP, 987-65-5; $bis_{22}ATP$ (3′ isomer), 104693-47-2; $bis_{22}ATP$ (2′ isomer), 104693-48-3; $bis_{22}ADP$ (3′ isomer), 104693-50-7; $bis_{22}ADP$ (2′ isomer), 104693-51-8; ATPase, 9000-83-3; $HO_2C(CH_2)_5NH_2$, 60-32-2.

REFERENCES

Ames, B. N., & Dubin, D. T. (1960) *J. Biol. Chem. 235*, 769–775.

Bachouchi, N., Gulik, A., Garrigos, M., & Morel, J. E. (1985) *Biochemistry 24*, 6305–6310.

Barden, J. A., & Mason, P. (1978) *Science (Washington, D.C.) 199*, 1212–1213.

Botts, J., Takashi, R., Torgerson, P., Hozumi, T., Muhlrad, A., Mornet, D., & Morales, M. F. (1984) *Proc. Natl. Acad. Sci. U.S.A. 81*, 2060–2064.

Ellman, G. L. (1959) *Arch. Biochem. Biophys. 82*, 70–77.

Garrigos, M., Morel, J. E., & Garcia de la Torre, J. (1983) *Biochemistry 22*, 4961–4969.

Goodno, C. C. (1979) *Proc. Natl. Acad. Sci. U.S.A. 76*, 2620–2624.

Gottikh, B. T., Krayevsky, A. A., Terussova, N. B., Purygin, P. P., & Tsilevich, J. L. (1970) *Tetrahedron 26*, 4419–4433.

Hansske, F., Sprinzl, M., & Cramer, F. (1974) *Bioorg. Chem. 3*, 367–376.

Harrington, W. F. (1971) *Proc. Natl. Acad. Sci. U.S.A. 68*, 685–689.

Harrington, W. F. (1979) *Proc. Natl. Acad. Sci. U.S.A. 76*, 5066–5070.

Highsmith, S., & Cooke, R. (1983) in *Cell and Muscle Motility* (Dowben, R., & Shay, J., Eds.) Vol. IV, pp 207–237, Plenum Press, New York.

Hiratsuka, T. (1984) *J. Biochem. 96*, 147–154.

Huxley, A. F. (1974) *J. Physiol. (London) 243*, 1–43.

Huxley, A. F., & Simmons, R. M. (1971) *Nature (London) 233*, 533–538.

Huxley, H. E. (1969) *Science (Washington, D.C.) 164*, 1356–1366.

Lamed, R., & Oplatka, A. (1974) *Biochemistry 13*, 3137–3142.

Lomant, A. J., & Fairbanks, G. (1976) *J. Mol. Biol. 104*, 243–261.

Lowey, S., Slater, H. S., Weeds, A. G., & Baker, H. J. (1969) *J. Mol. Biol. 42*, 1–29.

Mahoney, C. W., & Yount, R. G. (1984) *Anal. Biochem. 138*, 246–251.

Margossian, S. S., & Lowey, S. (1982) *Methods Enzymol. 85*, 55–71.

Margossian, S. S., Stafford, W. F., & Lowey, S. (1981) *Biochemistry 20*, 2151–2155.

Morales, M. F., Borejdo, J., Botts, J., Cooke, R., Mendelson, R. A., & Takashi, R. (1982) *Annu. Rev. Phys. Chem. 33*, 319–351.

Morel, J. E., & Garrigos, M. (1982) *Biochemistry 21*, 2679–2686.

Penefsky, H. (1977) *J. Biol. Chem. 252*, 2891–2897.

Rockstein, M., & Herron, P. W. (1951) *Anal. Chem. 23*, 1500–1505.

Sutoh, K., Yamamoto, K., & Wakabayashi, T. (1986) *Proc. Natl. Acad. Sci. U.S.A. 83*, 212–216.

Svedberg, T., & Pedersen, K. O. (1940) *The Ultracentrifuge*, Oxford University Press, New York.

Tonomura, Y., Imahura, K., Ikehara, M., Uno, H., & Harada, F. (1967) *J. Biochem. (Tokyo) 61*, 460–472.

Valentine, R. C., & Green, N. M. (1967) *J. Mol. Biol. 27*, 615–617.

Van Holde, K. E. (1967) *Sedimentation Equilibrium*, Fractions No. 1, Beckman Instruments, Palo Alto, CA.

Van Holde, K. E. (1971) *Physical Biochemistry*, Prentice-Hall, Englewood Cliffs, NJ.

Wagner, P. D., & Yount, R. G. (1975) *Biochemistry 14*, 1900–1907.

Wagner, P. D., & Weeds, A. G. (1977) *J. Mol. Biol. 109*, 445–473.

Weeds, A. G., & Taylor, R. S. (1975) *Nature (London) 257*, 54–56.

Wells, C., & Bagshaw, C. R. (1984) *J. Muscle Res. Cell Motil. 5*, 97–112.

Wells, J. A., & Yount, R. G. (1980) *Biochemistry 19*, 1711–1717.

Wells, J. A., Werber, M. M., & Yount, R. G. (1979) *Biochemistry 18*, 4800–4805.

Yang, J. T., & Wu, C. C. (1977) *Biochemistry 16*, 5785–5789.

Yphantis, D. A. (1964) *Biochemistry 3*, 297–317.